

Key Points:

- Melting of a metamorphosed basaltic crust on Venus at depths greater than 60 km and without water produces abundant felsic melts
- Felsic melts may have formed at various stages of crustal plateau evolution in diverse geodynamic settings and in the absence of water
- Partial melting produces residual eclogite in the crust that may delaminate and limit its thickness

Supporting Information:

Supporting Information may be found in the online version of this article.

Correspondence to:

M. Collinet,
max.collinet@unamur.be

Citation:

Collinet, M., Maia, J., Plesa, A.-C., Klemme, S., & Wieczorek, M. (2025). Felsic magmatism on Venus generated by crustal recycling and melting. *Journal of Geophysical Research: Planets*, 130, e2025JE009187. <https://doi.org/10.1029/2025JE009187>

Received 11 MAY 2025

Accepted 27 OCT 2025

Author Contributions:

Conceptualization: Julia Maia, Ana-Catalina Plesa, Mark Wieczorek
Funding acquisition: Ana-Catalina Plesa
Investigation: Max Collinet
Methodology: Max Collinet, Stephan Klemme
Resources: Ana-Catalina Plesa
Supervision: Ana-Catalina Plesa
Validation: Stephan Klemme
Visualization: Max Collinet, Julia Maia
Writing – original draft: Max Collinet, Julia Maia
Writing – review & editing: Julia Maia, Ana-Catalina Plesa, Stephan Klemme, Mark Wieczorek

© 2025. The Author(s).

This is an open access article under the terms of the [Creative Commons Attribution License](#), which permits use, distribution and reproduction in any medium, provided the original work is properly cited.

Felsic Magmatism on Venus Generated by Crustal Recycling and Melting

Max Collinet^{1,2} , Julia Maia² , Ana-Catalina Plesa² , Stephan Klemme³, and Mark Wieczorek⁴ 

¹Institute of Life, Earth and Environment (ILEE), University of Namur, Namur, Belgium, ²German Aerospace Center (DLR), Institute of Space Research, Berlin, Germany, ³Institute for Mineralogy, University of Muenster, Muenster, Germany, ⁴Université Paris Cité, Institut de physique du globe de Paris, CNRS, Paris, France

Abstract The observation of low viscosity lava flows and shield volcanoes on radar images, combined with X-ray fluorescence analyses performed by Soviet landers, strongly suggests that Venus's crust is primarily basaltic. However, near-infrared emissivity data from the Galileo and Venus Express missions indicate that crustal plateaus may be compositionally distinct and contain higher proportions of felsic minerals than the surrounding plains. The hypothesis that these highlands are felsic has led to suggestions of past oceans on Venus, as the generation of such rocks on Earth typically requires significant amounts of water. We use thermodynamic modeling to explore the conditions under which silica-rich melts can form without water, through deep melting of basaltic crust in thickened crustal roots or during crustal recycling in the mantle. Felsic melts containing 60–65 wt.% SiO₂ can form at depths >60 km. In regions of thickened crust, such melts would be produced along a thermal gradient of ~10 K/km, whereas for higher gradients (≥15 K/km), melting occurs at depths where quartz is not yet present (<50 km), resulting in silica-poor melts. The presence of small amounts of water allows similar felsic melts (in composition and volume) to form at moderately shallower depths (~40 km). Our results indicate that large volumes of felsic melt could form even under anhydrous conditions on Venus, via crustal thickening or recycling mechanisms such as subduction or lithospheric dripping. This supports the idea that part of Venus's highlands could be the product of remelted basaltic crust, regardless of whether surface water existed in the past.

Plain Language Summary Although most of the crust of Venus is thought to be made of basalt, like the Earth's oceanic crust, about 8% of its surface consists of elevated regions known as highlands or crustal plateaus, which have been proposed to resemble Earth's continental crust. On Earth, granite-rich continental crust forms when basalt interacts with liquid water and later melts again or is recycled at plate boundaries. Because of this, finding granites or other silica-rich rocks on Venus could suggest that the planet once had oceans. In this study, however, we show that silica-rich rocks can form without water, when basaltic crust melts deep below the surface, around 60 km depth. This process could occur at the base of locally thickened crust on Venus or within the mantle, when the crust sinks and is recycled by the planet's interior dynamics.

1. Introduction

Like most planetary bodies in the solar system, the crust of Venus appears to be predominantly composed of basalts (Basaltic Volcanism Study Project, 1981; Campbell & Taylor, 1983) and their weathering products (Dyar et al., 2021; Filiberto & McCanta, 2024; Semprich et al., 2020; Zolotov, 2018). Its surface is covered by volcanic terrains that are consistent with the outpouring of low viscosity basaltic flows (Gilmore et al., 2023; Head et al., 1992), which is likely still ongoing (Filiberto et al., 2020, 2025; Herrick et al., 2023; Smrekar et al., 2010). The rocks analyzed at several volcanic plains by the Venera and Vega landers are in line with orbital observations and resemble terrestrial tholeiites and alkali basalts (Filiberto, 2014; Surkov et al., 1984, 1986). Finally, major topographic rises on Venus associated with widespread volcanism and large gravity anomalies indicate that abundant plume activity could have fueled basaltic magmatism on Venus throughout most of its history (e.g., Mason et al., 2025; Smrekar et al., 2010; Stofan et al., 1995).

A type of highland on Venus, the so-called crustal plateaus, are heavily deformed, high-elevation regions that represent some of the planet's oldest surface units and bear a geomorphological resemblance with Earth's continental crust (Ivanov & Head, 1996). In addition, geophysical investigations indicate that they represent regions of thickened crust, with crustal thicknesses comparable to continents (Grimm, 1994; James et al., 2013; Maia &

Wieczorek, 2022; Simons et al., 1997). Near-infrared emissivity anomalies on the global (Hashimoto et al., 2008; Mueller et al., 2008) and regional scale (Gilmore et al., 2015) suggest that crustal plateaus on Venus may contain a greater fraction of felsic minerals than the surrounding basaltic lowlands. On Earth, however, felsic magmatism is associated with the breakdown of hydrated minerals in the crust, both in the Archean (Moyen & Martin, 2012) and at modern subduction zones (Grove et al., 2012). Furthermore, small volumes of felsic melt can also result from extensive fractional crystallization of water-poor basaltic melts on Earth and other planets (Grove & Brown, 2018; Jagoutz & Klein, 2018; Shellnutt, 2013; Udry et al., 2018), but this process is usually deemed insufficient to produce abundant felsic crusts on Venus in the absence of significant amounts of water (Gilmore et al., 2017; Shellnutt, 2018). Therefore, several authors assumed that the discovery of large volumes of intermediate to felsic rocks (i.e., andesitic to granitic) on Mars or Venus may indicate that hydrothermal alteration occurred at the bottom of water oceans on these planets in the past (Bernadet et al., 2025; Campbell & Taylor, 1983; Gilmore et al., 2023; Sautter et al., 2015).

Here, we propose mechanisms capable of generating substantial amounts of SiO_2 -rich melts on Venus with little to no water in the crust, eliminating the need to invoke water-rich conditions in the early stages of Venus's planetary evolution. We perform thermodynamic modeling (Connolly, 2009; Holland et al., 2018) to show that a Venusian basaltic crust contains quartz at depths in excess of 50–60 km and this allows for a large volume of felsic melt to be produced at these conditions. The onset of melting in basalts metamorphosed under granulite or eclogite facies conditions (hereafter referred to as metabasalts) under thickened crust was recently explored by Semprich et al. (2025) to define the petrological limits for the maximum crustal thickness of Venus. In this study, we investigate the conditions for crustal melting, the volumes of melt that can be produced, and their respective compositions. Additionally, we consider whether felsic crustal plateaus could be inherited from prior recycling and partial melting of the basaltic crust, which is likely to have occurred during Venus's evolution (e.g., Armann & Tackley, 2012; Davaille et al., 2017; Gölcher et al., 2020; Rolf et al., 2022).

2. Methods

We use the thermodynamic model of Holland et al. (2018) implemented in version 6.9.1 of Perple_X (Connolly, 2009) to calculate the phase proportions and compositions of metabasalts as a function of pressure and temperature by Gibbs-free energy minimization. The initial benchmarking performed by Holland et al. (2018) of the experiments of Pertermann and Hirschmann (2003) suggests that their melt solution model is applicable to basaltic compositions in the eclogite facies (at 3 GPa; see their figure 6). To confirm that the implementation of the Holland et al. (2018) model in our version of Perple_X is appropriate, we verify that the solidus temperature, phase proportions, and compositions from both series of experiments (G2 and G2K) can be predicted accurately (see Supporting Information S1). Finally, we compare the phase diagrams and, when available, the liquid compositions obtained with Perple_X to the ones of additional experimental studies (Green & Ringwood, 1972; Ito & Kennedy, 1971; Klemme et al., 2002; Rosenthal et al., 2018; Yaxley & Green, 1998).

Early experiments conducted to constrain the phase relations of anhydrous metabasalts (Green & Ringwood, 1972; Ito & Kennedy, 1971) showed that the positions of the basalt-granulite and granulite-eclogite facies limits are strongly dependent on the bulk composition of the rock considered (Green & Ringwood, 1972). The phase diagrams produced with Perple_X show a pressure of garnet appearance, which defines the basalt-granulite limit, spanning a pressure interval of 0.3 GPa (Figure 1), similar to the 0.3–0.4 GPa interval between the experimental phase diagram of Ito and Kennedy (1971) and Green and Ringwood (1972). Compared to these early experimental studies, relatively less variability is observed with Perple_X for the granulite-eclogite limit, defined by the disappearance of plagioclase feldspar (0.1 vs. 0.4 GPa interval). However, the average pressure of the limit is identical in experiments and thermodynamic calculations (e.g., 2.1 GPa at 1000°C; compare Figure 1 with Figure 1 of Green & Ringwood, 1972).

The early experiments by Ito and Kennedy (1971) and Green and Ringwood (1972) estimated solidus temperatures $\sim 100^\circ\text{C}$ higher than those calculated with Perple_X (e.g., 1285 vs. 1170°C at 3 GPa). Subsequent experimental work at similar pressures increasingly focused on hydrous basaltic systems (e.g., see the review by Moyen & Martin, 2012), with relatively few studies conducted on dry (nominally anhydrous) basaltic compositions (Klemme et al., 2002; Pertermann & Hirschmann, 2003; Rosenthal et al., 2018; Yaxley & Green, 1998). We calculated the solidus temperature with Perple_X for the five basaltic compositions used in these studies and found it to be accurate to within $\pm 20^\circ\text{C}$ to the experimentally constrained solidus for all but one composition:

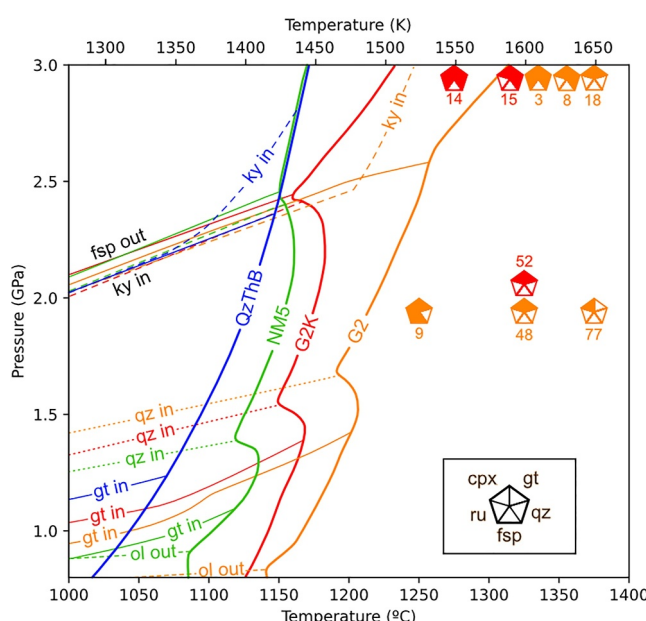


Figure 1. Simplified phase diagrams of four water-free terrestrial basaltic compositions used in experimental studies as calculated with Perple_X. QzThB—quartz tholeiite B (Green & Ringwood, 1972), NM5 (Ito & Kennedy, 1971), G2 and G2K (Pertermann & Hirschmann, 2003). Phase assemblage boundaries are labeled as qz (quartz), gt (garnet), ol (olivine), ky (kyanite), fsp (plagioclase feldspar), followed by “in” when the phase appears with increasing pressure or “out” when the phase disappears with increasing pressure. The fsp-out and ky-in boundaries show little dependence on the starting composition, which is why they are indicated with a black label. The experiments of Pertermann and Hirschmann (2003) for G2 (orange pentagons) and G2K (red pentagons) are represented with the melt fraction (in wt.%). See Figure S1 in Supporting Information S1 for a comparison of melt compositions and phase proportions. Additional phases present in experiments are ru (rutile) and cpx (clinopyroxene). The disappearance of plagioclase (fsp out) represents the transition into the eclogite facies. The appearance of garnet (gt in) represents the beginning of the granulite facies. Note that the “garnet in limit” varies more strongly with the bulk composition. Quartz appears with increasing pressure in the granulite facies (qz in), except for QzThB that is already saturated in quartz at lower pressure (quartz normative). The solidus curves (thick lines) are strongly dependent on composition. G2, a potassium-poor basalt has the highest solidus temperatures.

Res3 in Rosenthal et al. (2018). In this last study, the solidus was lower by $\sim 50^{\circ}\text{C}$ than our Perple_X calculations. The majority of experimental studies are in agreement with the solidus temperatures calculated by Perple_X (Klemme et al., 2002; Pertermann & Hirschmann, 2003; Yaxley & Green, 1998), with the remaining ones showing either higher (Green & Ringwood, 1972; Ito & Kennedy, 1971) or lower (Rosenthal et al., 2018) solidus temperatures. Therefore, we consider that the thermodynamic calculations used in this study are appropriate to estimate solidus temperatures with an accuracy that falls within the range of the inter-laboratory reproducibility. The mineral phase assemblages and melt compositions (including the SiO_2 concentration) calculated with Perple_X are also consistent with existing experimental studies (and in particular Pertermann & Hirschmann, 2003, see Supporting Information S1).

As these tests are deemed successful, we apply the same method to model the mineralogy and melting behavior of all Venusian basaltic compositions measured in situ by X-ray fluorescence at the Venera 13, 14, and Vega 2 landing sites (Surkov et al., 1984, 1986). In doing so, we assume that any of these compositions may be representative of the crust of Venus and discuss phase transformations and partial melting at depth. Sulfur and chlorine were excluded before re-normalizing the compositions to 100 wt.% as these elements are not included in the Holland et al. (2018) model and might in part result from superficial alteration on the surface of Venus (Table S1 in Supporting Information S1). While Venus appears to have lost a substantial amount of water (Kasting & Pollack, 1983), the mantle might still contain hundreds of ppm of water (e.g., Elkins-Tanton et al., 2007; Greenwood et al., 2018) and primary basaltic melts were likely never entirely anhydrous. Thus, we also calculated phase relations for Vega 2 with 0.5 and 1.0 wt.% H_2O added, which could reasonably be obtained without invoking hydrothermal alteration at the bottom of an ocean, in order to investigate the influence of moderate water concentrations on the melting behavior and melt compositions. We apply a pressure to depth conversion assuming an average density of 3100 kg/m^3 for a pore-free crust, which is consistent with Perple_X calculations (see Section 3), down to a depth of 100 km (2.75 GPa). To calculate density contrasts between the crust and the mantle, we assume a composition equal to the fertile terrestrial peridotite KLB-1 (Takahashi, 1986). The detailed settings and initial files that were used for Perple_X calculations are available in Supporting Information S1.

3. Results

3.1. Phase Equilibria and Limits on Crustal Thickness

The phase diagrams produced for the basaltic compositions analyzed by the Vega 2 and Venera 14 landers are nearly identical (Figure 2), and similar to the ones of terrestrial tholeiites (Figure 1). The low-pressure phase assemblage (< 0.5 GPa, see Figure 3) contains around 60 wt.% plagioclase, orthopyroxene and clinopyroxene (for a total of 25–30 wt.%), olivine (5 wt.% in Venera 14 and 15 wt.% in Vega 2), and accessory spinel and ilmenite (in Venera 14 only). The pressure of quartz appearance is slightly lower for Venera 14 than for Vega 2 (1.15 vs. 1.35 GPa at 1000°C). The subsolidus high-pressure mineral assemblages (ca. 2.5 GPa; Figure 2 and Figure S2 in Supporting Information S1) are typical of quartz-eclogites: clinopyroxene (omphacite), garnet, kyanite, and quartz. The solidus temperatures are also similar and, for example, equal to 1130°C (Vega 2) and 1150°C (Venera 14) at 2 GPa. The maximum depths of neutral buoyancy ($\rho_{\text{mantle}} = \rho_{\text{crust}}$) are not rigorously identical and occur at 67 km for Vega 2 and at 85 km for Venera 14, corresponding to thermal gradients of 10 and 8.5 K/km, respectively (Figure 2). The maximum depth of neutral buoyancy can be understood as the maximum crustal thickness that can be sustained for a given

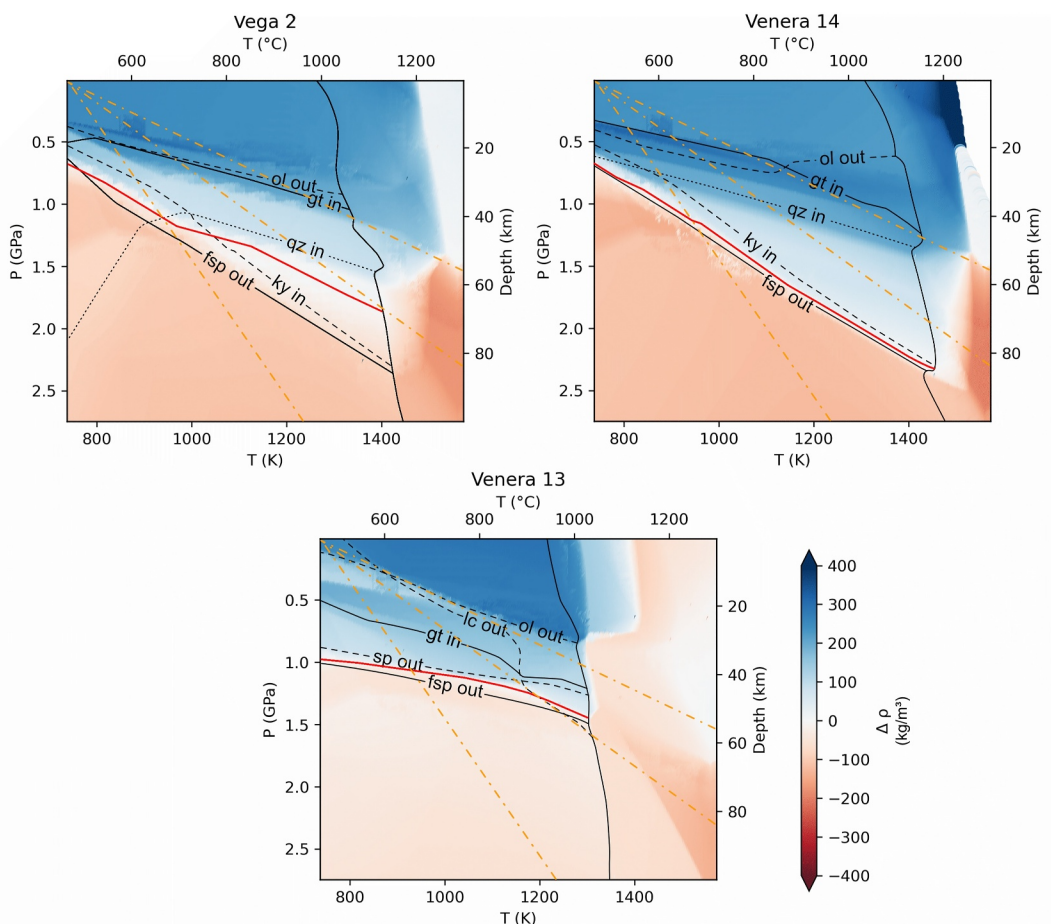


Figure 2. Simplified phase diagrams for the Venusian basaltic compositions Vega 2, Venera 13 and Venera 14. Phase boundaries are annotated following Figure 1. The solidus is the steep black curve. The orange dash-dotted lines indicate, from left to right, the 5, 10, and 15 K/km thermal gradients, which bracket the likely present-day regional variations (e.g., Bjornnes et al., 2021; Maia et al., 2025, and references therein). The color scale represents the density contrast between the mantle and basaltic crust, assuming a composition equivalent to the one of Vega 2, Venera 13 or Venera 14, respectively. The crust is denser than the mantle when the values are negative (red colors). The position of neutral buoyancy is represented by the solid red line, which largely coincides with the eclogite transition (i.e., the fsp out boundary). Note that Venera 13 is quartz-undersaturated and contains leucite (lc) and kalsilite (kls) at low pressure.

composition if it were limited by density. A crust of composition identical to that of samples analyzed by Vega 2 would, for instance, become denser than the mantle at depths shallower than 67 km and cold thermal gradients below 10 K/km. At higher thermal gradients, crustal melting is initiated at shallower depths, and the resulting solid residue (restite) quickly exceeds the density of the underlying mantle (Figure 2, see also Semprich et al. (2025) for a discussion of the relationship between maximum crustal thickness and thermal gradients).

The phase diagram of the alkali basalt analyzed by the Venera 13 lander strongly contrasts with the ones of the two tholeiitic basalts (Venera 14 and Vega 2). The Venera 13 composition remains quartz-undersaturated even at high pressures. The basaltic assemblage contains plagioclase, clinopyroxene, olivine, and nepheline with accessory ilmenite and spinel, while the eclogitic assemblage only contains three phases: clinopyroxene (omphacite), garnet, and kalsilite. The pressures of the garnet-in and plagioclase-out transitions are much closer to each other (1.2 and 1.45 GPa at 1000°C, respectively). The solidus temperature is 40–80°C lower than the solidus of Venera 14 and Vega 2 (e.g., 1065°C instead of 1130–1150 at 2 GPa) and the maximum depth of neutral buoyancy is also lower: 55 km, corresponding to a thermal gradient of 11 K/km, in agreement with Semprich et al. (2025).

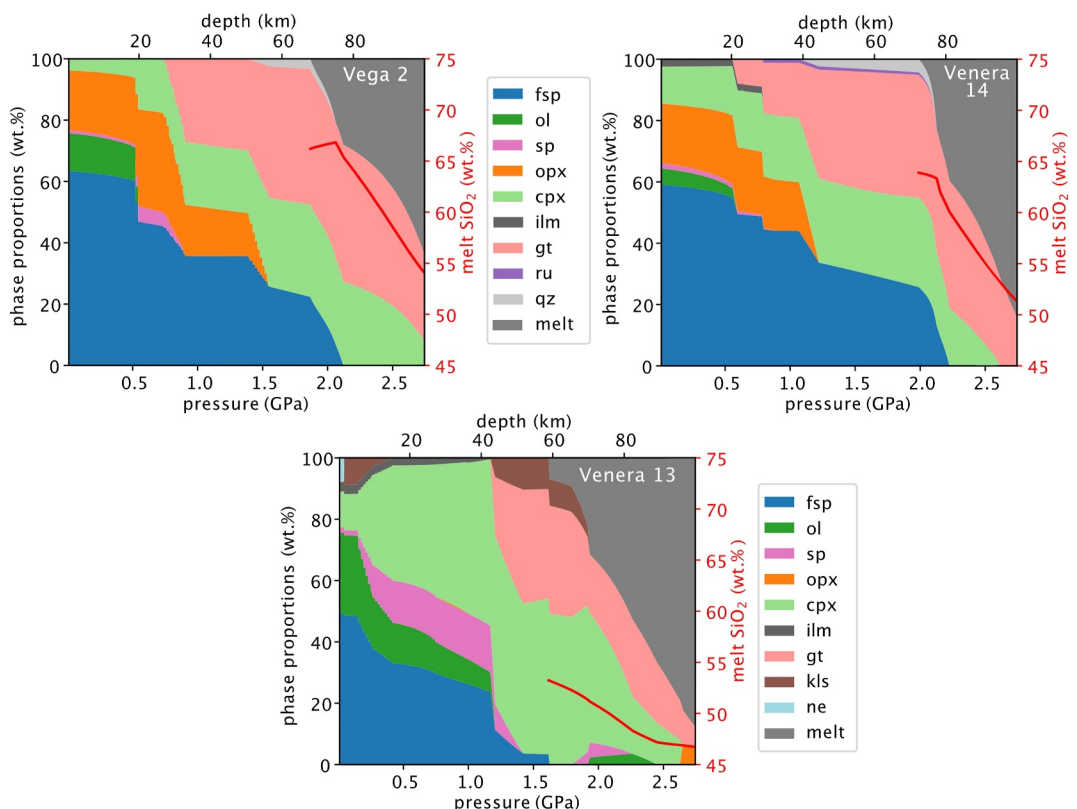


Figure 3. Evolution of mineral proportions with increasing pressure and temperature along the 10 K/km gradient (middle orange dashed-dotted line of Figure 2), for Vega 2, Venera 14 and Venera 13. The red line (and related values on the right hand y-axis) depicts the SiO_2 concentration of the melt when it is present (above the solidus). Note that melting begins before the eclogite transition for Vega 2 and Venera 14, in the presence of both feldspar and quartz. Quartz is not present in Venera 13, and, consequently, the resulting silicate melt is poor in SiO_2 compared to the melts produced from Vega 2 and Venera 14.

3.2. Crustal Anatexis and Melt Compositions

The melting behavior of the Venusian crust at high pressure is first examined along the 10 K/km thermal gradient. Despite uncertainty and model dependence, this represents the value toward which most estimates for average present-day Venus converge (e.g., Bjonnes et al., 2021; Borrelli et al., 2021; Maia et al., 2025). Along this gradient, the solidus is reached at a depth of 59, 67, and 72 km, for Venera 13, Vega 2, and Venera 14 compositions, respectively (Figure 3). Plagioclase and quartz (for Venera 14 and Vega 2) or kalsilite (for Venera 13) are quickly consumed by the melting reactions, which also involve a small fraction of clinopyroxene. For Vega 2 and Venera 14, quartz is the first phase to melt out (at 75–77 km) and is followed by plagioclase (77–81 km) and clinopyroxene at much larger depths (95–105 km). By the time quartz disappears, the melt fractions reach 21 and 23 wt.%. They reach 28–39 wt.% when plagioclase is fully consumed and 70 wt.% when clinopyroxene is removed from the residue. The SiO_2 content peaks at 64–66 wt.% when quartz disappears, then gradually declines as lower SiO_2 phases, such as omphacite, are progressively incorporated into the melt. The Venera 13 composition does not contain quartz and, therefore, the melts that are produced along the 10 K/km geotherm are much poorer in SiO_2 (<54 wt.%).

As melting progresses, the density of the solid residue increases rapidly (Figure 4) due to the disappearance of the low-density phases plagioclase and quartz. The solid residue becomes denser than the mantle close to the solidus temperature and the density contrast ($\sim 200 \text{ kg/m}^3$) becomes constant after the complete disappearance of plagioclase. At that point, at a depth of ~ 80 km, the melt is $\sim 700 \text{ kg/m}^3$ less dense than the residual eclogite and 500 kg/m^3 less dense than the mantle. The density contrast between the residual eclogite and the mantle ($\sim 200 \text{ kg/m}^3$) is similar to the density contrast that develops along smaller thermal gradients (e.g., 5 K/km), where the crust reaches the eclogite facies without melting ($\sim 170 \text{ kg/m}^3$; Figure S4 in Supporting Information S1).

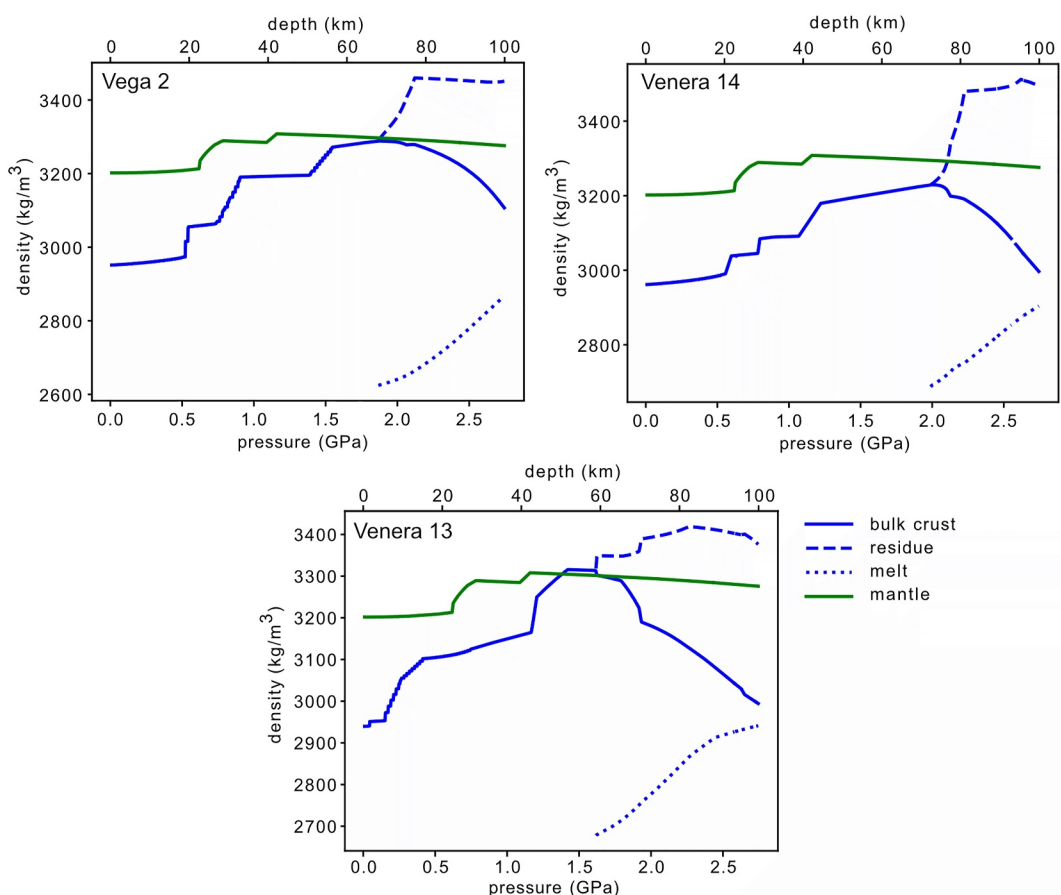


Figure 4. Evolution of the density of the crust, assuming compositions identical to Vega 2, Venera 14, and Venera 13 along the 10 K/km thermal gradient compared to the density of the mantle (KLB-1; Takahashi, 1986). Note that for all three compositions, partial melting results in a residue that is substantially denser than the mantle.

The influence of quartz on the composition of partial melts is also clear in Figure 5. At pressures lower than ~ 1.3 GPa (and depths less than 50 km), little to no quartz is present in the mineral assemblage when the crust reaches its solidus temperature. The SiO_2 content of the melt quickly increases from 51 wt.% (mafic) at 1.2 GPa to more than 65 wt.% (felsic) at 1.4–1.5 GPa, including at low melt fraction (Figure 5a), following the appearance of quartz. The proportion of quartz in the crust continues to increase slowly with pressure and larger amounts of SiO_2 -rich melts can thus be produced at 70–80 km. At these depths, the fraction of felsic melts (63–64 wt.% SiO_2) can easily reach 25 wt.%. At low pressure (< 0.3 GPa, < 10 km), the SiO_2 concentration of the melts also increases despite the absence of quartz. At these shallow conditions, melting is incongruent and results in the production of a substantial proportion of olivine (Figure S7 in Supporting Information S1), leading to the production of a melt that is more enriched in silica, but intermediate rather than felsic ($55 \text{ wt.\%} < \text{SiO}_2 < 60 \text{ wt.\%}$). Reaching partial melting at these shallow depths would require extreme thermal gradients approaching 80–100 K/km, which have, however, been proposed during tesserae formation (Resor et al., 2021).

The addition of 0.5 and 1 wt.% H_2O to the Vega 2 basalt illustrates how melting a hydrated basaltic crust can facilitate the production of felsic material. The solidus is lowered by up to a few hundred degrees (Figure 5c) and quartz becomes stable at lower pressure (Figure S6 in Supporting Information S1). As a result, limited amounts of SiO_2 -rich melts can be produced at shallower depths, with a peak of 71 wt.% at 1 GPa (36 km) for a 5 wt.% melt fraction (Figure 5a). On the other hand, larger fractions of felsic melts remain limited to higher pressures (> 1.15 GPa), in the stability field of garnet (Figure 5e). When the basaltic crust is hydrated, up to 25 wt.% felsic melt can form at depths as shallow as ~ 50 km, in contrast to ~ 70 km under anhydrous conditions (Figure 5f).

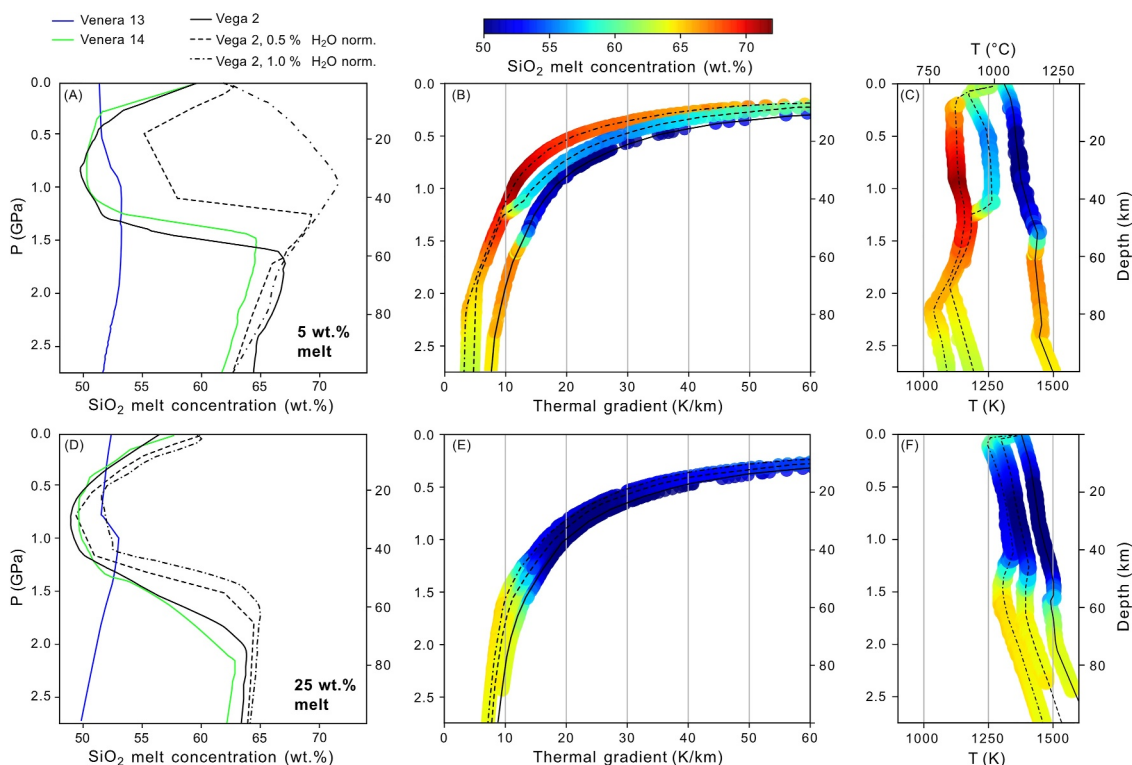


Figure 5. SiO_2 concentration at fixed melt fractions (5 wt.% or 25 wt.%) and increasing pressures and depths (a and d), corresponding thermal gradients required to reach a melt fraction of 5 or 25 wt.% for the Vega 2 composition (b and e), and corresponding temperature of formation for the 5 and 25 wt.% Vega 2 melts (c and f). Melts produced at pressures above 1.5 GPa (depth greater than 55 km) are SiO_2 -rich (62–66 wt.%), except if the bulk composition is alkali-rich and SiO_2 under-saturated like Venera 13. The effect of 0.5 and 1.0 wt.% H_2O (dashed line and dash-dotted line, respectively) is illustrated for Vega 2. For low degrees of melting (5 wt.%), water increases the SiO_2 content of the melts at low pressure. For larger degrees of melting (25 wt.%), water has a negligible effect on the melt composition (d) but still lowers the temperature at which they can be produced by up to 200 K (f). For a given thermal gradient (e.g., 10–12 K/km), moderate amounts of water thus lower the depth at which large fractions of felsic melts can be produced by 15–20 km (e).

4. Discussion

4.1. Deeply Sourced Felsic Melts: Venusian Plateaus Compared to the Earth's Early Continental Crust

The partial melting of metabasalts was likely frequent on Earth during the Archean (and possibly Hadean) eons due to the higher mantle temperatures and heat fluxes. Archean cratons that form the core of continents are largely made of intermediate to felsic rocks belonging to the so-called Tonalites-Trondhjemites-Granodiorites (TTG) suite and associated “gray gneisses” (Laurent et al., 2024; Moyen & Martin, 2012). Among other distinctive features, they are characterized by large fractions of sodic feldspar and low abundances of heavy rare earth elements compared to the more recent potassic granites formed since the Archean. As with most terrestrial felsic rocks, water played a key role in the formation of TTGs. When incorporated into hydrous minerals that form during alteration of basaltic crust, it lowers the solidus temperature of subducting metabasalts by several hundred degrees, facilitating the production of large fractions of felsic material across a broad range of pressures. In comparison, although relatively few studies have examined the melting of dry metabasalts at high pressure, some suggest that this process would be ineffective on Earth, instead producing a few percent of potassic granites at most (Moyen & Martin, 2012). However, both the experiments of Pertermann and Hirschmann (2003) and the modeling performed on Venusian tholeiites (Venera 14 and Vega 2) show that large fractions of felsic magmas can also be produced at sufficiently high pressures and temperatures in the absence of water (Figure 5).

The major element compositions of high-degree (25 wt.%) melts produced from dry metabasalts are nearly identical to those of melts generated at lower temperatures from a hydrated crust (Figure 6f). Although strictly granitic melts can only be produced at relatively low pressure (1 GPa) from a hydrated basaltic crust (Figures 5a and 6a), the dacitic-trachytic melts produced in large quantity at high pressure can easily reach SiO_2 contents of 65–70 wt % following modest degrees of fractional crystallization. Such felsic rocks would plot on the tonalite–

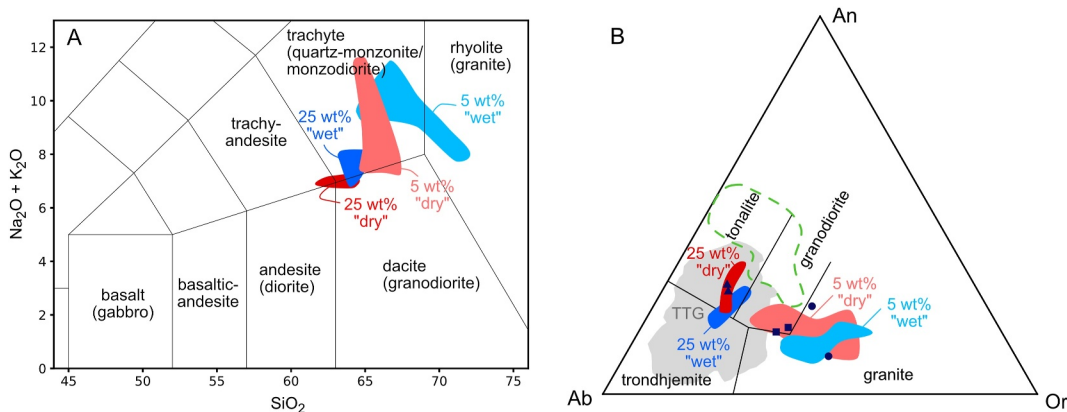


Figure 6. Major element composition of modeled partial melts for the Vega 2 basaltic composition with 1.0 wt.% H_2O (“wet”) and no water (“dry”) sampled irrespectively of the depth of melting from Figure 5, but keeping only melts with $\text{SiO}_2 > 62$ wt.%. (a) Total alkali-silica diagram. Note that high- SiO_2 “wet” melts correspond to the ~ 1 GPa peak SiO_2 of Figure 5a. (b) Normative Anorthite–Albite–Orthoclase triangle comparing modeled melts to the global distribution of Archean TTGs (gray field; Moyen & Martin, 2012). The experimental melts from Wang et al. (2022) based on a synthetic basalt of composition identical to Venera 14 are contoured by the green dashed line. Note however that the high An content of these compositions likely results from an analytical artifact as relatively high current intensities (12 nA) and a focused beam (1 μm) was used for EPMA analyses, causing Na-mobility during measurements (Wang et al., 2022). The dark blue symbols (triangles, squares, and circles) are the experimental melts with > 61 wt.% SiO_2 from Pertermann and Hirschmann (2003), Yaxley and Green (1998), and Klemme et al. (2002), respectively. Note that the major element composition of melts produced in the presence or absence of anhydrous minerals are nearly indistinguishable.

trondhjemite–granodiorite triple point in the distinctive ternary feldspar diagram (Figure 6b), despite having been produced from a water-poor basaltic crust. On Earth, identifying TTGs formed in different geodynamic environments is notoriously difficult and relies on trace element concentrations that are indicative of the presence of certain indicator minerals (e.g., plagioclase, garnet, amphibole, and rutile) in the residue (Moyen, 2011). If significant volumes of felsic material were confirmed on Venus—for instance, at crustal plateaus—constraining the conditions of its formation, including the role of water, would be difficult given the limited petrological and geochemical data available. However, considering Venus elevated surface and interior temperatures, as well as the potential for crustal recycling under hypothesized tectonic regimes (see next section), the generation of TTG-like rocks could have been possible even in the absence of water. Wang et al. (2022) also explored this possibility experimentally, although, in detail, their melt compositions are more enriched in SiO_2 and depleted in Na_2O compared to both our modeled compositions and the experimental melts obtained for terrestrial compositions (e.g., Pertermann & Hirschmann, 2003) at similar pressure and temperature conditions (Figure 6b). The origin of this discrepancy is unknown and additional experiments could help characterize the nature of deeply sourced felsic melts under anhydrous to moderately hydrated conditions.

4.2. Geodynamic Settings

First, we evaluate whether felsic melts can be produced in a setting similar to that of present-day Venusian crustal plateaus. This possibility was already mentioned by Hess and Head (1990) who suggested that melting dry metabasalts in the crustal roots of plateaus could form felsic melts based on a single experiment from Johnston (1986) and geological observations consistent with the presence of thickened crust in orogenic belts (e.g., Crumpler et al., 1986). Several studies later confirmed that crustal plateaus and Ishtar Terra are associated with crustal thickening (e.g., Grimm, 1994; James et al., 2013; Maia & Wieczorek, 2022; Simons et al., 1997) using gravity and topography data from the Magellan mission. In particular, Maia and Wieczorek (2022) found that the crustal thickness of Ovda Regio could currently reach up to 55 km, while Maxwell Montes, at Ishtar Terra, is probably the region with thickest crust on the planet, potentially reaching over 70 km (Hansen & Phillips, 1995; James et al., 2013; Jiménez-Díaz et al., 2015). At crustal plateaus, thermal gradients are likely variable and most constraints suggest values higher than the global average of ~ 10 K/km. Fold modeling predicts that, depending on the choice of flow laws, thermal gradients higher than 25–40 K/km were required at the time of their formation (e.g., Brown & Grimm, 1997; Resor et al., 2021). Thermal gradients derived from estimates of the lithospheric

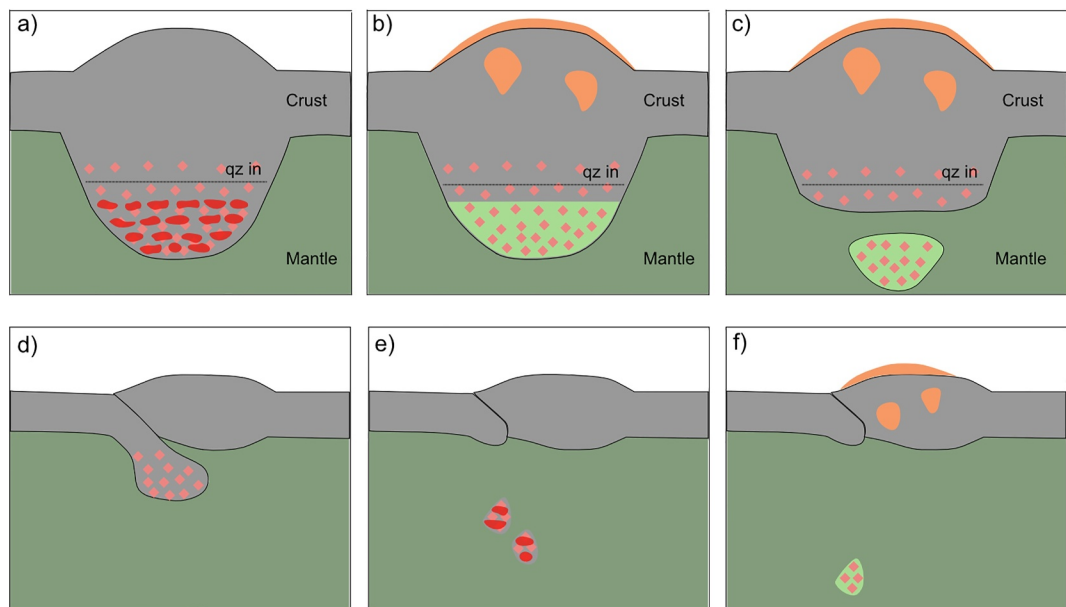


Figure 7. Geodynamic settings of possible felsic melt formation by deep melting of anhydrous to “wet” (1 wt.% H_2O) metabasalts. Top panels (a–c): melting at the base of the crust starts (red pockets) in the presence of quartz and garnet (pink diamonds), where the crustal thickness reaches 40–55 km (for a “wet” or anhydrous basaltic composition, respectively). Following partial melting, the felsic melts rise toward the upper crust and crystallize (orange) while the residual lower crust (restite, light green) becomes eclogitic (b) and can delaminate (c). This scenario can explain the formation of felsic crustal plateaus thicker than 40 km (e.g., Ovda). The large crustal thickness suspected at Maxwell Montes (~70 km) could indicate that partial melting is ongoing at this location (a) that delamination was hindered (b) or that the lower crust has a distinct composition (e.g., ultra-mafic and Al-poor). Bottom panels (d–f): local subduction or large-scale resurfacing brings eclogite deeper in the mantle, allowing it to melt in the presence of quartz, for example, as crustal material sinks into the mantle (e). The felsic melt is extracted to the upper crust while the residual eclogite continues to sink in the mantle (f).

elastic thickness are, on average, lower (in the range 10–15 K/km), yet remain compatible with fold modeling estimates within the large model uncertainties (see Section 4.2 in Maia & Wieczorek, 2022). We note that, while high thermal gradients (>40 K/km) might have occurred early during tesserae formation, they cannot be sustained or easily extrapolated at depths larger than 20 km as the crust would reach near total melting (Figure S6 in Supporting Information S1). If such gradients affected the upper part of the crust only (e.g., the first 10 km), large volumes of intermediate (55–60 wt.% SiO_2) magma compositions could have been produced but not strictly felsic in composition (defined as > 63–65 wt.% SiO_2) (Figure 5d). Flexural studies suggest that thermal gradients exceeding 20 K/km may be locally confined to the lithosphere beneath coronae and rift zones, likely due to underlying thermal anomalies (O’Rourke & Smrekar, 2018; Smrekar et al., 2023). For the remainder of the discussion, we assume that gradients as low as 10–15 K/km existed during or soon after the formation of crustal plateaus, as they are more compatible with the large crustal thickness estimates (Maia & Wieczorek, 2022; Ruiz, 2007).

At the root of Maxwell Montes (up to 70 km depth), large volumes (ca. 25 wt.%) of dacitic melts are expected to be generated, if the base of the crust is metabasaltic (granulite to eclogite facies), for thermal gradients of 10–11 K/km. Note that with thermal gradients higher than 11 K/km, a metabasaltic crust would melt before reaching a depth of 70 km (see also Semprich et al., 2025). At Ovda Regio, partial melting is expected to occur at the base of the crust (i.e., at 55 km depth) for thermal gradients of 12–14 K/km (Figure 5), which generally overlaps with the range of thermal gradient estimates based on the elastic thickness at this location (Maia & Wieczorek, 2022). At a depth of 55 km, only a few percent of felsic melt (63–64 wt.% SiO_2) can be generated (Figures 5a–5c) and the melt would quickly become intermediate at higher temperature (Figures 5d–5f; 56–57 wt.% SiO_2). As melting proceeds and quartz and feldspar are consumed, residual eclogites are produced and the remaining crust becomes denser than the mantle (Figures 2 and 3). Therefore, it is possible that partial melting initially occurred at an average depth substantially larger than the maximum crustal thickness subsisting at Ovda today (e.g., 60–70 km, Figure 7a), thus producing large fractions of dacitic melts (ca. 25 wt.%) that could have risen toward the surface

(Figure 7b), while the residual eclogite founded (Figure 7c). Note that, while this mechanism could account for the emplacement of felsic batholiths and lava flows at Ovda, it is not incompatible with the outpouring of mantle-sourced mafic magmas (Wroblewski et al., 2019) as delamination of the melting residue in the crust could trigger a return flow in the asthenosphere, leading to decompression melting.

If a small fraction of water were locked within hydrous minerals in the basaltic crust (e.g., 0.5–1.0 wt.% bulk H_2O), quartz would appear at shallower conditions, thus producing large fractions of felsic melts at lower depth (i.e., 40–50 km). The effect of water would also lower the solidus by a couple hundred of degrees (Figure 5c). With 1.0 wt.% water, only a few percent of felsic melt can be produced at low pressure (depth <40 km; Figures 5a and 5b), before the melt becomes basaltic in composition (Figures 5d and 5e). Thermal gradients <14 K/km and depths in excess of 40 km are therefore still required to produce larger fractions of dacitic melts (25 wt.%; Figure 5e) that would be easier to extract from the lower crust (McKenzie, 1985).

In summary, felsic melts could have formed in the current configuration of crustal plateaus, where the crustal thickness reached 40–60 km, if the lower crust was moderately hydrated (up to 1 wt.% H_2O) or dry, respectively. The crustal thickness could be limited to ~50 km, for example, at Ovda, by partial melting and subsequent recycling of the residue (see also Semprich et al., 2025). However, some plateaus may have never attained such large crustal thickness. For instance, Alpha Regio—the only plateau suspected to be felsic based on currently available near-infrared emissivity data (Gilmore et al., 2015)—does not exhibit significant crustal thickness today, and it is possible that its crust was never sufficiently thick to support felsic melt production by partial melting of its root. Alternative crustal recycling mechanisms would thus be required to account for the origin of abundant felsic rocks at crustal plateaus with a crustal thickness of 30 km and under.

We note that under low thermal gradients (5–7 K/km), crustal delamination would likely precede the onset of partial melting, but would still require depths greater than 40 km (Figure 2). Delamination could bring basaltic material deeper into the mantle, allowing it to melt at a depth larger than 60 km to produce abundant felsic melts. However, delamination prior to partial melting would require low thermal gradients (i.e., about 5–7 K/km), which are below the vast majority of thermal gradient estimates for Venus (Bjornes et al., 2021; Borrelli et al., 2021; O'Rourke & Smrekar, 2018) and for plateaus in particular (Maia & Wieczorek, 2022; Resor et al., 2021). In addition, even if such low thermal gradients were relevant for crustal plateaus, they would be associated with a thicker lithosphere that might prevent crustal delamination (Breuer & Spohn, 2006; Plesa & Breuer, 2014). However, under dynamic conditions such as subduction initiation or a plume-assisted delamination, transient low thermal gradients may have appeared.

Several studies suggest that tesserae, as the stratigraphically oldest terrains on the planet, could be witnesses of an earlier, perhaps more tectonically active, phase of Venus's evolution—one that preceded large-scale resurfacing events during which portions of the crust were extensively recycled (e.g., Gilmore & Head, 2018; Karlsson et al., 2020; Romeo & Turcotte, 2008; Tian et al., 2023; Turcotte et al., 1999). Crustal recycling may also still occur on regional scales. This has been proposed by global geodynamic models advocating for a “plutonic-squishy lid” tectonic regime (e.g., Lourenço et al., 2020; Rolf et al., 2022), as well as by regional models and laboratory experiments suggesting active lithospheric subduction at some coronae (e.g., Davaille et al., 2017; Gölcher et al., 2020). Therefore, it is clear that crustal recycling plays an important role in the planet's geodynamic evolution and that there should have been numerous opportunities for generating felsic melts by partial melting of metabasalts at depth. Partial melts would not remain trapped in the descending, partly molten, basaltic crust but instead rise back to the surface (Figures 7d–7f), even for water-poor and relatively viscous dacitic melts (Elkins-Tanton et al., 2007).

4.3. No Water, No Granite?

A key objective of the upcoming VERITAS (Smrekar et al., 2022), EnVision (Straume-Lindner et al., 2022), and DAVINCI (Garvin et al., 2022) missions is to determine whether Venusian crustal plateaus are composed of felsic material, or if the observed near-infrared emissivity anomalies can be explained by alternative causes, such as the presence of low-emissivity alteration minerals (Gilmore et al., 2015, 2017). At present, these anomalies are thought to result from a primary (igneous) mineralogy with low FeO content, as alteration is not expected to be sufficiently pervasive to completely modify the surface spectra (Dyar et al., 2021; Gilmore et al., 2023). If future missions confirm widespread felsic material at crustal plateaus, it may support the idea of past water oceans, as melting of hydrated basalts, together with the igneous differentiation of hydrous melts, are considered an effective

way to generate large volumes of felsic melt on Venus, Earth or any rocky planet (Campbell & Taylor, 1983; Gilmore et al., 2023; Grove et al., 2012; Hashimoto et al., 2008; Jagoutz & Klein, 2018; Laurent et al., 2024; Moyen & Martin, 2012). However, alternative mechanisms may account for the widespread occurrence of felsic lithologies.

On Earth, while the oceanic crust can reach 6 wt.% H₂O (Tamblyn et al., 2023), normal mid-oceanic ridge basalts contain 0.2 wt.% H₂O on average prior to their hydrothermal alteration (Danyushevsky, 2001). Most chondritic materials contain substantial water, including EH chondrites that could share similarities with the building blocks of Mercury, Venus, and the Earth (Piani et al., 2020). Upon melting, they could easily generate basaltic melts containing a couple of percent of water. However, a large fraction of the planetesimals that formed the terrestrial planets may have melted and dehydrated prior to their final accretion (Peterson et al., 2025), suggesting that Venus, positioned closer to the Sun, likely received less water than the Earth during late accretion (Gillmann et al., 2020). However, even if the overall amount of water trapped in Venus's mantle were small, it is conceivable that percent levels of H₂O accumulated over time in the lithosphere and lower crust due to metasomatic processes (Elkins-Tanton et al., 2007). Hence, we surmise that we cannot exclude small to moderate concentrations of water (estimated at a few hundreds to a few thousands of ppm of water) in the basaltic crust of Venus, even if it never interacted with surface water.

Felsic material could also be produced incrementally by fractional crystallization of basaltic melts with no or minimal water (0.2 wt.%, Shellnutt, 2013). In this case, only a limited volume of felsic material (up to 10 wt.% of the initial basaltic melt) can be produced (e.g., Jagoutz & Klein, 2018; Shellnutt, 2018). Although it may be sufficient to produce viscous steep-sided domes locally on Venus (Cao et al., 2025), this process would likely not be able to fully cover large regions of the crust and could not account for the formation of crustal plateaus, if they were confirmed to be predominantly felsic.

However, in this work, we show clearly that melting of anhydrous metabasaltic crust at high pressure in the two geodynamics settings described in the previous section (Figure 7) is perfectly suitable to produce large volumes of felsic melts. The presence of minor to moderate water in the crust (< 1 wt.%) only relaxes the minimum pressure at which this process can occur and facilitates melt extraction due to its viscosity lowering effect (e.g., Giordano et al., 2008). Even dry dacitic melts are expected to be efficiently extracted from Venus's interior. Despite their high viscosity, their low density facilitates ascent, while the residual eclogite, being denser, can be recycled into the mantle (see Stokes velocity calculations in Elkins-Tanton et al. (2007) and Figure 4). Largely anhydrous felsic (dacitic) material at crustal plateaus would also enable them to maintain their steep topography over billion-year timescales more easily than if they contained substantial fractions of hydrous granites (Nimmo & Maxwell, 2023). While the exact geodynamic setting in which crustal plateaus formed on Venus is debated—potentially involving either lateral or vertical tectonic processes (Bindschadler & Head, 1991; Capitanio et al., 2024), and echoing a similar debate for the formation of the early continental crust on Earth (e.g., Arndt, 2023; Capitanio et al., 2019)—most scenarios are compatible with the formation of abundant felsic material without requiring surface water-rock interaction.

5. Conclusions

Results from thermodynamic modeling show that large amounts of silica-rich melts (60–65 wt.%) can be generated on Venus by melting of anhydrous metabasalts at depths larger than 55 km, where quartz becomes stable (granulite or eclogite facies). These conditions can be reached either (a) directly at the base of the crust, under several crustal plateaus and tesserae complexes (e.g., Ovda and Maxwell Montes), and assuming a geothermal gradient of 8–12 K/km or (b) through local or global resurfacing events, which would inevitably involve crustal recycling and partial melting at depth, given the lower solidus temperature of basalt relative to peridotite.

If thermal gradients were higher (>15 K/km) at the base of crustal plateaus, melting would occur before quartz forms, and, consequently, the resulting melts would contain only low amounts of silica (<55 wt.%). Although water lowers the pressure and temperature required to generate felsic melts, it does not significantly affect the total melt volume or the major-element composition of melts produced at depths greater than 55–60 km.

Conflict of Interest

The authors declare no conflicts of interest relevant to this study.

Data Availability Statement

All data presented in this manuscript is available in Supporting Information S1 repository on Zenodo (Collinet et al., 2025).

Acknowledgments

ACP and SK acknowledge funding from the Deutsche Forschungsgemeinschaft (DFG, German Research Foundation)—Project-ID 509061759. JM acknowledges support from the Alexander von Humboldt Foundation. We thank C.J. Renggli, L. Jennings, E.S. Steenstra and G. Golabek for insightful discussions about Venus. We thank two anonymous reviewers for their thoughtful comments that helped to improve an earlier version of this manuscript and the editor Debra Buczkowski for handling our paper. Open Access funding enabled and organized by Projekt DEAL.

References

Armann, M., & Tackley, P. J. (2012). Simulating the thermochemical magmatic and tectonic evolution of Venus's mantle and lithosphere: Two-dimensional models. *Journal of Geophysical Research*, 117(E12). <https://doi.org/10.1029/2012JE004231>

Arndt, N. (2023). How did the continental crust form: No basalt, no water, no granite. *Precambrian Research*, 397, 107196. <https://doi.org/10.1016/j.precamres.2023.107196>

Basaltic Volcanism Study Project. (1981). *Basaltic volcanism on the terrestrial planets* (p. 1286). Pergamon Press, Inc. New York.

Bernadet, J., Borisova, A. Y., Guitreau, M., Safonov, O. G., Asimow, P., Nédélec, A., et al. (2025). Making continental crust on water-bearing terrestrial planets. *Science Advances*, 11(13), eads6746. <https://doi.org/10.1126/sciadv.ads6746>

Bindschadler, D. L., & Head, J. W. (1991). Tessera terrain, Venus: Characterization and models for origin and evolution. *Journal of Geophysical Research*, 96(B4), 5889–5907. <https://doi.org/10.1029/90JB02742>

Björnnes, E., Johnson, B. C., & Evans, A. J. (2021). Estimating Venusian thermal conditions using multiring basin morphology. *Nature Astronomy*, 5, 498–502. <https://doi.org/10.1038/s41550-020-01289-6>

Borrelli, M. E., O'Rourke, J. G., Smrekar, S. E., & Ostberg, C. M. (2021). A global survey of lithospheric flexure at steep-sided domical volcanoes on Venus reveals intermediate elastic thicknesses. *Journal of Geophysical Research: Planets*, 126(7), e2020JE006756. <https://doi.org/10.1029/2020JE006756>

Breuer, D., & Spohn, T. (2006). Viscosity of the Martian mantle and its initial temperature: Constraints from crust formation history and the evolution of the magnetic field. *Planetary and Space Science*, 54(2), 153–169. <https://doi.org/10.1016/j.pss.2005.08.008>

Brown, C. D., & Grimm, R. E. (1997). Tessera deformation and the contemporaneous thermal state of the Plateau Highlands, Venus. *Earth and Planetary Science Letters*, 147(1–4), 1–10. [https://doi.org/10.1016/S0012-821X\(97\)00007-1](https://doi.org/10.1016/S0012-821X(97)00007-1)

Campbell, I. H., & Taylor, S. R. (1983). No water, no granites—No oceans, no continents. *Geophysical Research Letters*, 10(11), 1061–1064. <https://doi.org/10.1029/GL010p01061>

Cao, R., Saper, L. M., Bromiley, G. D., Antoshechkina, P. M., & Law, S. (2025). Formation of steep-sided domes on Venus via eruption of high crystallinity magmas. *Icarus*, 433, 116524. <https://doi.org/10.1016/j.icarus.2025.116524>

Capitanio, F. A., Kerr, M., Stegman, D. R., & Smrekar, S. E. (2024). Ishtar terra highlands on Venus raised by craton-like formation mechanisms. *Nature Geoscience*, 17(8), 740–746. <https://doi.org/10.1038/s41561-024-01485-3>

Capitanio, F. A., Nebel, O., Cawood, P. A., Weinberg, R. F., & Chowdhury, P. (2019). Reconciling thermal regimes and tectonics of the early Earth. *Geology*, 47(10), 923–927. <https://doi.org/10.1130/G46239.1>

Collinet, M., Maia, J., Plesa, A.-C., Klemme, S., & Wieczorek, M. (2025). Felsic magmatism on Venus generated by deep crustal melting [Dataset]. Zenodo. <https://doi.org/10.5281/zenodo.15374491>

Connolly, J. A. (2009). The geodynamic equation of state: What and how. *Geochemistry, Geophysics, Geosystems*, 10. <https://doi.org/10.1029/2009GC002540>

Crumpler, L. S., Head, J. W., & Campbell, D. B. (1986). Orogenic belts on Venus. *Geology*, 14, 1031–1034. [https://doi.org/10.1130/0091-7613\(1986\)14<1031:OBOV>2.0.CO;2](https://doi.org/10.1130/0091-7613(1986)14<1031:OBOV>2.0.CO;2)

Danyushevsky, L. V. (2001). The effect of small amounts of H₂O on crystallisation of mid-ocean ridge and backarc basin magmas. *Journal of Volcanology and Geothermal Research*, 110(3–4), 265–280. [https://doi.org/10.1016/S0377-0273\(01\)00213-X](https://doi.org/10.1016/S0377-0273(01)00213-X)

Davaille, A., Smrekar, S. E., & Tomlinson, S. (2017). Experimental and observational evidence for plume-induced subduction on Venus. *Nature Geoscience*, 10(5), 349–355. <https://doi.org/10.1038/geo2928>

Dyar, M. D., Helbert, J., Cooper, R. F., Sklute, E. C., Maturilli, A., Mueller, N. T., et al. (2021). Surface weathering on Venus: Constraints from kinetic, spectroscopic, and geochemical data. *Icarus*, 358, 114139. <https://doi.org/10.1016/j.icarus.2020.114139>

Elkins-Tanton, L. T., Smrekar, S. E., Hess, P. C., & Parmentier, E. M. (2007). Volcanism and volatile recycling on a one-plate planet: Applications to Venus. *Journal of Geophysical Research*, 112(E4). <https://doi.org/10.1029/2006JE002793>

Filiberto, J. (2014). Magmatic diversity on Venus: Constraints from terrestrial analog crystallization experiments. *Icarus*, 231, 131–136. <https://doi.org/10.1016/j.icarus.2013.12.003>

Filiberto, J., & McCanta, M. C. (2024). Characterizing basalt-atmosphere interactions on Venus: A review of thermodynamic and experimental results. *American Mineralogist*, 109(5), 805–813. <https://doi.org/10.2138/am-2023-9015>

Filiberto, J., Trang, D., Treiman, A. H., & Gilmore, M. S. (2020). Present-day volcanism on Venus as evidenced from weathering rates of olivine. *Science Advances*, 6(1), eaax7445. <https://doi.org/10.1126/sciadv.aax7445>

Filiberto, J., Zolotov, M. Y., Kohler, E., D'Incecco, P., Gorinov, D. A., Bhiravarasu, S. S., et al. (2025). Assessing the evidence for active volcanism on Venus: Current limitations and prospects for future investigations. *Geochemistry*, 126316. <https://doi.org/10.1016/j.chemer.2025.126316>

Garvin, J. B., Getty, S. A., Arney, G. N., Johnson, N. M., Kohler, E., Schwer, K. O., et al. (2022). Revealing the mysteries of Venus: The davinci mission. *The Planetary Science Journal*, 3(5), 117. <https://doi.org/10.3847/psj/ac63c2>

Gillmann, C., Golabek, G. J., Raymond, S. N., Schönbächler, M., Tackley, P. J., Dehant, V., & Debaille, V. (2020). Dry late accretion inferred from Venus's coupled atmosphere and internal evolution. *Nature Geoscience*, 13(4), 265–269. <https://doi.org/10.1038/s41561-020-0561-x>

Gilmore, M. S., Dyar, M. D., Mueller, N., Brossier, J., Santos, A. R., Ivanov, M., et al. (2023). Mineralogy of the Venus surface. *Space Science Reviews*, 219(7), 52. <https://doi.org/10.1007/s11214-023-00988-6>

Gilmore, M. S., & Head, J. W. (2018). Morphology and deformational history of Tellus Regio, Venus: Evidence for assembly and collision. *Planetary and Space Science*, 154, 5–20. <https://doi.org/10.1016/j.pss.2018.02.001>

Gilmore, M. S., Mueller, N., & Helbert, J. (2015). Virtis emissivity of alpha Regio, Venus, with implications for Tessera composition. *Icarus*, 254, 350–361. <https://doi.org/10.1016/j.icarus.2015.04.008>

Gilmore, M. S., Treiman, A., Helbert, J., & Smrekar, S. E. (2017). Venus surface composition constrained by observation and experiment. *Space Science Reviews*, 212(3–4), 1511–1540. <https://doi.org/10.1007/s11214-017-0370-8>

Giordano, D., Russell, J. K., & Dingwell, D. B. (2008). Viscosity of magmatic liquids: A model. *Earth and Planetary Science Letters*, 271(1–4), 123–134. <https://doi.org/10.1016/j.epsl.2008.03.038>

Green, D. H., & Ringwood, A. E. (1972). A comparison of recent experimental data on the Gabbro–Garnet Granulite–eclogite transition. *The Journal of Geology*, 80(3), 277–288. <https://doi.org/10.1086/627731>

Greenwood, J. P., ichiro Karato, S., Kaaden, K. E. V., Pahlevan, K., & Usui, T. (2018). Water and volatile inventories of Mercury, Venus, the Moon, and Mars. *Space Science Reviews*, 214(5), 92. Netherlands. <https://doi.org/10.1007/s11214-018-0526-1>

Grimm, R. E. (1994). The deep structure of Venusian Plateau Highlands. *Icarus*, 112(1), 89–103. <https://doi.org/10.1006/icar.1994.1171>

Grove, T. L., & Brown, S. M. (2018). Magmatic processes leading to compositional diversity in igneous rocks: Bowen (1928) revisited. *American Journal of Science*, 318, 1–28. <https://doi.org/10.2475/01.2018.02>

Grove, T. L., Till, C. B., & Krawczynski, M. J. (2012). The role of H_2O in subduction zone magmatism. *Annual Review of Earth and Planetary Sciences*, 40(1), 413–439. <https://doi.org/10.1146/annurev-earth-042711-105310>

Gülcher, A. J. P., Gerya, T. V., Montési, L. G. J., & Munch, J. (2020). Corona structures driven by plume–lithosphere interactions and evidence for ongoing plume activity on Venus. *Nature Geoscience*, 13(8), 547–554. <https://doi.org/10.1038/s41561-020-0606-1>

Hansen, V. L., & Phillips, R. J. (1995). Formation of Ishtar Terra, Venus: Surface and gravity constraints. *Geology*, 23, 292–296. [https://doi.org/10.1130/0091-7613\(1995\)023\(0292:FOITVS\)2.3.CO;2](https://doi.org/10.1130/0091-7613(1995)023(0292:FOITVS)2.3.CO;2)

Hashimoto, G. L., Roos-Serote, M., Sugita, S., Gilmore, M. S., Kamp, L. W., Carlson, R. W., & Baines, K. H. (2008). Felsic highland crust on Venus suggested by Galileo near-infrared mapping spectrometer data. *Journal of Geophysical Research*, 113(E5). <https://doi.org/10.1029/2008je003134>

Head, J. W., Crumpler, L. S., Aubele, J. C., Guest, J. E., & Saunders, R. S. (1992). Venus volcanism: Classification of volcanic features and structures, associations, and global distribution from Magellan data. *Journal of Geophysical Research*, 97(E8), 13153–13197. <https://doi.org/10.1029/92JE01273>

Herrick, R. R., Bjornes, E. T., Carter, L. M., Gerya, T., Ghail, R. C., Gillmann, C., et al. (2023). Resurfacing history and volcanic activity of Venus. *Space Science Reviews*, 219(4), 29. <https://doi.org/10.1007/s11214-023-00966-y>

Hess, P. C., & Head, J. W. (1990). Derivation of primary magmas and melting of crustal materials on Venus: Some preliminary petrogenetic considerations. *Earth, Moon, and Planets*, 50–51(1), 57–80. <https://doi.org/10.1007/bf00142389>

Holland, T. J. B., Green, E. C. R., & Powell, R. (2018). Melting of peridotites through to granites: A simple thermodynamic model in the system KNCFMASHTOCr. *Journal of Petrology*, 59(5), 881–900. <https://doi.org/10.1093/petrology/egy048>

Ito, K., & Kennedy, G. C. (1971). An experimental study of the Basalt–Garnet Granulite–Eclogite transition. In *The structure and physical properties of the Earth's crust* (pp. 303–314). <https://doi.org/10.1029/GM014p0303>

Ivanov, M. A., & Head, J. W. (1996). Tessera terrain on Venus: A survey of the global distribution, characteristics, and relation to surrounding units from Magellan data. *Journal of Geophysical Research*, 101(E6), 14861–14908. <https://doi.org/10.1029/96JE01245>

Jagoutz, O., & Klein, B. (2018). On the importance of crystallization–differentiation for the generation of SiO_2 –Rich melts and the compositional build-up of arc (and continental) crust. *American Journal of Science*, 318(1), 29–63. <https://doi.org/10.2475/01.2018.03>

James, P. B., Zuber, M. T., & Phillips, R. J. (2013). Crustal thickness and support of topography on Venus. *Journal of Geophysical Research: Planets*, 118(4), 859–875. <https://doi.org/10.1029/2012je004237>

Jiménez-Díaz, A., Ruiz, J., Kirby, J. F., Romeo, I., Tejero, R., & Capote, R. (2015). Lithospheric structure of Venus from gravity and topography. *Icarus*, 260, 215–231. <https://doi.org/10.1016/j.icarus.2015.07.020>

Johnston, A. D. (1986). Anhydrous p-t phase relations of near-primary high-alumina basalt from the South Sandwich Islands. *Contributions to Mineralogy and Petrology*, 92(3), 368–382. <https://doi.org/10.1007/BF00572166>

Karlsson, R. V., Cheng, K. W., Cramer, F., Rolf, T., Uppalapati, S., & Werner, S. C. (2020). Implications of anomalous crustal provinces for Venus' resurfacing history. *Journal of Geophysical Research: Planets*, 125(10), e2019JE006340. <https://doi.org/10.1029/2019JE006340>

Kasting, J. F., & Pollack, J. B. (1983). Loss of water from Venus. I. Hydrodynamic escape of hydrogen. *Icarus*, 53(3), 479–508. [https://doi.org/10.1016/0019-1035\(83\)90212-9](https://doi.org/10.1016/0019-1035(83)90212-9)

Klemme, S., Blundy, J. D., & Wood, B. J. (2002). Experimental constraints on major and trace element partitioning during partial melting of eclogite. *Geochimica et Cosmochimica Acta*, 66(17), 3109–3123. [https://doi.org/10.1016/S0016-7037\(02\)00859-1](https://doi.org/10.1016/S0016-7037(02)00859-1)

Laurent, O., Guitreau, M., Bruand, E., & Moyen, J.-F. (2024). At the dawn of continents: Archean tonalite–trondhjemite–granodiorite suites. *Elements*, 20(3), 174–179. <https://doi.org/10.2138/gselements.20.3.174>

Lourenço, D. L., Rozel, A. B., Ballmer, M. D., & Tackley, P. J. (2020). Plutonic–squishy lid: A new global tectonic regime generated by intrusive magmatism on Earth-like planets. *Geochemistry, Geophysics, Geosystems*, 21(4), e2019GC008756. <https://doi.org/10.1029/2019GC008756>

Maia, J. S., Plesa, A.-C., van Zelst, I., Ghail, R., Gülcher, A. J. P., Panning, M. P., et al. (2025). The seismogenic thickness of Venus. *Journal of Geophysical Research: Planets*, 130(7), e2025JE009065. <https://doi.org/10.1029/2025JE009065>

Maia, J. S., & Wieczorek, M. A. (2022). Lithospheric structure of Venusian crustal plateaus. *Journal of Geophysical Research: Planets*, 127(2), e2021JE007004. <https://doi.org/10.1029/2021je007004>

Mason, P. J., Kildaras, A., Cirium, D., Ghail, R. C., & Lea-Wurzbach, S. (2025). Evolution of plume volcanism at Atla Regio, Venus. *Journal of Geophysical Research: Planets*, 130(2), e2024JE008815. <https://doi.org/10.1029/2024JE008815>

McKenzie, D. (1985). The extraction of magma from the crust and mantle. *Earth and Planetary Science Letters*, 74(1), 81–91. [https://doi.org/10.1016/0012-821X\(85\)90168-2](https://doi.org/10.1016/0012-821X(85)90168-2)

Moyen, J. F. (2011). The composite Archean grey gneisses: Petrological significance, and evidence for a non-unique tectonic setting for Archean crustal growth. *Lithos*, 123(1–4), 21–36. <https://doi.org/10.1016/j.lithos.2010.09.015>

Moyen, J. F., & Martin, H. (2012). Forty years of TTG research. *Lithos*, 148, 312–336. <https://doi.org/10.1016/j.lithos.2012.06.010>

Mueller, N., Helbert, J., Hashimoto, G. L., Tsang, C. C. C., Erard, S., Piccioni, G., & Drossart, P. (2008). Venus surface thermal emission at 1 μm in virtis imaging observations: Evidence for variation of crust and mantle differentiation conditions. *Journal of Geophysical Research*, 113(E5). <https://doi.org/10.1029/2008je003118>

Nimmo, F., & Mackwell, S. (2023). Viscous relaxation as a probe of heat flux and crustal plateau composition on Venus. *Proceedings of the National Academy of Sciences*, 120(3), e2216311120. <https://doi.org/10.1073/pnas.2216311120>

O'Rourke, J. G., & Smrekar, S. E. (2018). Signatures of lithospheric flexure and elevated heat flow in stereo topography at coronae on Venus. *Journal of Geophysical Research: Planets*, 123(2), 369–389. <https://doi.org/10.1002/2017JE005358>

Pertermann, M., & Hirschmann, M. M. (2003). Anhydrous partial melting experiments on MORB-like eclogite: Phase relations, phase compositions and mineral–melt partitioning of major elements at 2–3 GPa. *Journal of Petrology*, 44(12), 2173–2201. <https://doi.org/10.1093/petrology/egg074>

Peterson, L. D., Newcombe, M. E., Alexander, C. M., Wang, J., & Nielsen, S. G. (2025). A reconstruction of the H₂O and f contents of the ERG CECH 002 parent body. *Geochimica et Cosmochimica Acta*, 399, 82–92. <https://doi.org/10.1016/j.gca.2025.04.009>

Piani, L., Marrocchi, Y., Rigaudier, T., Vacher, L. G., Thomassin, D., & Marty, B. (2020). Earth's water may have been inherited from material similar to enstatite chondrite meteorites. *Science*, 369(6507), 1110–1113. <https://doi.org/10.1126/science.aba1948>

Plesa, A.-C., & Breuer, D. (2014). Partial melting in one-plate planets: Implications for thermo-chemical and atmospheric evolution. *Planetary and Space Science*, 98, 50–65. <https://doi.org/10.1016/j.pss.2013.10.007>

Resor, P. G., Gilmore, M. S., Straley, B., Senske, D. A., & Herrick, R. R. (2021). Felsic tesserae on Venus permitted by lithospheric deformation models. *Journal of Geophysical Research: Planets*, 126(4), e2020JE006642. <https://doi.org/10.1029/2020JE006642>

Rolf, T., Weller, M., Gölcher, A., Byrne, P., O'Rourke, J. G., Herrick, R., et al. (2022). Dynamics and evolution of Venus' mantle through time. *Space Science Reviews*, 218(8), 70. <https://doi.org/10.1007/s11214-022-00937-9>

Romeo, I., & Turcotte, D. (2008). Pulsating continents on Venus: An explanation for crustal plateaus and tessera terrains. *Earth and Planetary Science Letters*, 276(1–2), 85–97. <https://doi.org/10.1016/j.epsl.2008.09.009>

Rosenthal, A., Yaxley, G. M., Crichton, W. A., Kovács, I. J., Spandler, C., Hermann, J., et al. (2018). Phase relations and melting of nominally “dry” residual eclogites with variable CaO/Na₂O from 3 to 5 GPa and 1250 to 1500°C; implications for refertilisation of upwelling heterogeneous mantle. *Lithos*, 314–315, 506–519. <https://doi.org/10.1016/j.lithos.2018.05.025>

Ruiz, J. (2007). The heat flow during the formation of ribbon terrains on Venus. *Planetary and Space Science*, 55(14), 2063–2070. <https://doi.org/10.1016/j.pss.2007.05.003>

Sautter, V., Toplis, M. J., Wiens, R. C., Cousin, A., Fabre, C., Gasnault, O., et al. (2015). In situ evidence for continental crust on early Mars. *Nature Geoscience*, 8, 605–609. <https://doi.org/10.1038/ngeo2474>

Semprich, J., Filiberto, J., & Treiman, A. H. (2020). Venus: A phase equilibria approach to model surface alteration as a function of rock composition, oxygen- and sulfur fugacities. *Icarus*, 346, 113779. <https://doi.org/10.1016/j.icarus.2020.113779>

Semprich, J., Filiberto, J., Weller, M., Gorce, J., & Clark, N. (2025). Metamorphism of Venus as driver of crustal thickness and recycling. *Nature Communications*, 16(1), 2905. <https://doi.org/10.1038/s41467-025-58324-1>

Shellnutt, J. G. (2013). Petrological modeling of basaltic rocks from Venus: A case for the presence of silicic rocks. *Journal of Geophysical Research: Planets*, 118(6), 1350–1364. <https://doi.org/10.1002/jgre.20094>

Shellnutt, J. G. (2018). Derivation of intermediate to silicic magma from the basalt analyzed at the Vega 2 Landing Site, Venus. *PLoS One*, 13(3), e0194155. <https://doi.org/10.1371/journal.pone.0194155>

Simons, M., Solomon, S., & Hager, B. (1997). Localization of gravity and topography: Constraints on the tectonics and mantle dynamics of Venus. *Geophysical Journal International*, 131(1), 24–44. <https://doi.org/10.1111/j.1365-246x.1997.tb00593.x>

Smrekar, S. E., Hensley, S., Nybakken, R., Wallace, M. S., Perkovic-Martin, D., You, T.-H., et al. (2022). Veritas (Venus emissivity, radio science, InSAR, topography, and spectroscopy): A discovery mission. In 2022 IEEE Aerospace Conference (AERO) (pp. 1–20). <https://doi.org/10.1109/AERO53065.2022.9843269>

Smrekar, S. E., Ostberg, C., & O'Rourke, J. G. (2023). Earth-like lithospheric thickness and heat flow on Venus consistent with active rifting. *Nature Geoscience*, 16(1), 13–18. <https://doi.org/10.1038/s41561-022-01068-0>

Smrekar, S. E., Stofan, E. R., Mueller, N., Treiman, A., Elkins-Tanton, L., Helbert, J., et al. (2010). Recent hotspot volcanism on Venus from virtis emissivity data. *Science*, 328(5978), 605–608. <https://doi.org/10.1126/science.1186785>

Stofan, E. R., Smrekar, S. E., Bindschadler, D. L., & Senske, D. A. (1995). Large topographic rises on Venus: Implications for mantle upwelling. *Journal of Geophysical Research*, 100(E11), 23317–23327. <https://doi.org/10.1029/95je01834>

Straume-Lindner, A.-G., Buchwald, R., Crouzet, P.-E., Titov, D., Voirin, T., & Wielders, A. (2022). Envision: An ESA medium-class mission to Venus in collaboration with NASA. In *EPSC abstracts*. <https://doi.org/10.5194/epsc2022-196>

Surkov, Y. A., Barsukov, V. L., Moskalyeva, L. P., Kharyukova, V. P., & Kemurdzhian, A. L. (1984). New data on the composition, structure, and properties of Venus rock obtained by Venera 13 and Venera 14. *Journal of Geophysical Research*, 89(S02), B393–B402. <https://doi.org/10.1029/JB089iS02p0B393>

Surkov, Y. A., Moskalyova, L. P., Kharyukova, V. P., Dudin, A. D., Smirnov, G. G., & Zaitseva, S. Y. (1986). Venus rock composition at the Vega 2 landing site. *Journal of Geophysical Research*, 91(B13), E215–E218. <https://doi.org/10.1029/JB091iB13p0E215>

Takahashi, E. (1986). Melting of a dry peridotite klb-1 up to 14 GPa: Implications on the origin of peridotitic upper mantle. *Journal of Geophysical Research*, 91(B9), 9367–9382. <https://doi.org/10.1029/JB091iB09p09367>

Tamblyn, R., Hermann, J., Hasterok, D., Sossi, P., Pettke, T., & Chatterjee, S. (2023). Hydrated komatiites as a source of water for ttg formation in the Archean. *Earth and Planetary Science Letters*, 603, 117982. <https://doi.org/10.1016/j.epsl.2022.117982>

Tian, J., Tackley, P., & Lourenço, D. (2023). The tectonics and volcanism of Venus: New modes facilitated by realistic crustal rheology and intrusive magmatism. *Icarus*, 399, 115539. <https://doi.org/10.1016/j.icarus.2023.115539>

Turcotte, D. L., Morein, G., Roberts, D., & Malamud, B. D. (1999). Catastrophic resurfacing and episodic subduction on Venus. *Icarus*, 139(1), 49–54. <https://doi.org/10.1006/icar.1999.6084>

Udry, A., Gazel, E., & McSween, H. Y. (2018). Formation of evolved rocks at gale crater by crystal fractionation and implications for Mars crustal composition. *Journal of Geophysical Research: Planets*, 123(6), 1525–1540. <https://doi.org/10.1029/2018JE005602>

Wang, Y. J., Shellnutt, J. G., Kung, J., Iizuka, Y., & Lai, Y. M. (2022). The formation of tonalitic and granodioritic melt from Venusian basalt. *Scientific Reports*, 12(1), 1652. <https://doi.org/10.1038/s41598-022-05745-3>

Wroblewski, F. B., Treiman, A. H., Bhiravarasu, S., & Gregg, T. K. (2019). Ovda fluctus, the festoon lava flow on Ovda Regio, Venus: Not silica-rich. *Journal of Geophysical Research: Planets*, 124(8), 2233–2245. <https://doi.org/10.1029/2019JE006039>

Yaxley, G. M., & Green, D. H. (1998). Reactions between eclogite and peridotite: Mantle refertilisation by subduction of oceanic crust. *Schweizerische mineralogische und petrographische Mitteilungen*, 78, 243–255.

Zolotov, M. Y. (2018). 10. Gas–solid interactions on Venus and other solar system bodies. In P. King, B. Fegley, & T. Seward (Eds.), *High temperature gas-solid reactions in Earth and planetary processes* (pp. 351–392). De Gruyter. Berlin, Boston. <https://doi.org/10.1515/rmg.2018.84.10>